Procedia Computer Science
Volume 29, 2014, Pages 769–778
ICCS 2014. 14th International Conference on Computational Science

Nested Space Mapping Technology for Expedite EM-driven Design of Compact RF/microwave Components

Adrian Bekasiewicz[1*], Slawomir Koziel[2†], Piotr Kurgan[1‡], and Leifur Leifsson[2§]
[1]*Gdansk University of Technology, Poland*
[2]*Reykjavik University, Iceland*
adrian.bekasiewicz@eti.pg.gda.pl, koziel@ru.is, piotr.kurgan@eti.pg.gda.pl, leifurth@ru.is

Abstract
A robust simulation-driven methodology for rapid and reliable design of RF/microwave circuits comprising compact microstrip resonant cells (CMRCs) is presented. We introduce a nested space mapping (NSM) technology, in which the inner space mapping layer is utilized to improve the generalization capabilities of the equivalent circuit model corresponding to a constitutive element of the circuit under consideration. The outer layer enhances the surrogate model of the entire structure under design. We demonstrate that NSM significantly improves performance of surrogate-based optimization of composite RF/microwave structures. It is validated using two examples of UWB microstrip matching transformers (MTs) and compared to other competitive surrogate-assisted methods attempting to solve the problem of compact RF/microwave component design.

Keywords: EM-driven design, space mapping, compact RF components, design optimization

1 Introduction

The ability to rapidly and accurately design RF/microwave passives meeting the stringent requirements of space-limited applications is an important challenge of modern wireless communication engineering. Conventional RF/microwave components are simply too large for the use in miniaturization-oriented applications (especially in the lower parts of the spectrum), yet necessary for proper operation of wireless communication systems. To address this issue, numerous works, e.g., (Tsai 2013; Kurgan *et al.*, 2012; Wincza and Gruszczynski, 2013; Chuang and Wu, 2004; Smierzchalski *et al.* 2010; Kurgan and Kitlinski, 2010), proposed redesign of conventional

[*] Faculty of Electronics, Telecommunications and Informatics
[†] Engineering Optimization & Modeling Center, School of Science and Engineering
[‡] Faculty of Electronics, Telecommunications and Informatics
[§] Engineering Optimization & Modeling Center, School of Science and Engineering

Selection and peer-review under responsibility of the Scientific Programme Committee of ICCS 2014

doi:10.1016/j.procs.2014.05.069

RF/microwave components by replacing their fundamental building blocks, i.e., uniform transmission lines (UTLs), with composite structures of increased complexity. Geometrical parameters of these structures have to be adjusted to yield a compact design with a satisfactory performance. Although finding an abbreviated substitute for a UTL can be achieved by means of simplified transmission line theory with negligible numerical effort (e.g., Kurgan and Kitlinski, 2009; Bekasiewicz and Kurgan, 2014), subsequent optimization of a highly-compressed and complex circuit layout has been considered an extremely challenging problem. The main reason is the necessity of using accurate, but CPU-intensive electromagnetic (EM) simulation tools for reliable evaluation of the component's performance, but also a large number of designable parameters that increase the complexity of the optimization task. As opposed to conventional RF/microwave components, their miniaturized counterparts are computationally much more expensive, which is another important factor hindering the design process. For these reasons, classical EM-driven approaches of obtaining a final design, based either on laborious parameter sweeps (usually one parameter at a time) guided by engineering experience or a direct optimization, are found to be of limited use or even prohibitive when applied to numerically demanding RF/microwave components with complex topologies that are described by multiple designable parameters (Koziel *et al*., 2011; Koziel *et al*., 2013a; Koziel and Ogurstov, 2013).

The main drawback of a direct (e.g., gradient-based) EM optimization, which lies in a high computational cost of the process, can be mitigated to some extent by using surrogate-based optimization (SBO) techniques (Bandler *et al*., 2004; Koziel *et al*., 2013a; Koziel *et al*., 2013b) that shift the computational burden from iterative evaluation of a numerically demanding EM model to a computationally cheap low-fidelity surrogate exploited in an iterative prediction-correction loop. For the past years, the SBO concept has proven its vital usefulness in a multitude of instances, e.g. (Cheng et al., 2006; Koziel *et al*., 2006; Forrester and Keane, 2009; Koziel and Ogurstov, 2012), showcasing a cost-efficient handling of complex optimization problems described by a relatively small number of independent variables and supplied with well-suited physics-based analytical models of good generalization capabilities available for conventional RF/microwave components. In case of compact RF/microwave components with complex topologies, analytical coarse models are highly inaccurate and their utilization causes convergence problems of the SBO process (Koziel *et al*., 2008).

In (Bekasiewicz *et al.*, 2012), a method based on the design problem decomposition and a SBO concept has been proposed to address the obstacle of a large number of designable parameters and a high computational cost of the design, yielding satisfactory design solutions of RF/microwave components with complex topologies at a relatively small cost. However, this technique requires an inconvenient manual setup of multiple optimization problems, which circumvents the necessity of handling a large number of parameters in a single optimization attempt.

In (Kurgan and Bekasiewicz, 2014), an extension to the method of (Bekasiewicz *et al.*, 2012) has been reported and validated using an extremely complex optimization problem with a few dozens of designable parameters. By fixing a number of geometrical variables on the basis of theoretical premises and low-cost preliminary studies of a low-fidelity model, a successful optimization was performed. This approach enables to deal with a few dozens of optimization variables in a numerically efficient manner, but is hindered by the same drawback as method (Bekasiewicz *et al.*, 2012).

In this work, we propose a nested space mapping (NSM) approach for rapid design of compact RF/microwave components based on compact microstrip resonant cells (CMRCs). NSM constructs a two-stage surrogate model, with the inner SM layer applied at the level of the decomposed components of the structure under consideration, and the outer SM layer applied for the entire circuit. NSM addressed the problem of inaccurate surrogate models for compact RF/compact components by ensuring their excellent generalization capabilities, which results not only in rapid design improvement but also enables to solve the problem in a single optimization attempt. Our technique is demonstrated using several UWB microstrip MTs and compared with two benchmark surrogate-based optimization methods.

2 Nested Space Mapping Modeling

In this section, a nested space mapping (NSM) methodology is formulated. We also demonstrate its importance for ensuring good generalization of SM-based surrogate models of CMRC structures, as well as NSM advantages over conventional SM modeling.

2.1 Formulation of the Design Problem

Let $\boldsymbol{R}_f$ denote the response vector of a EM-simulated model of the CMRC structure of interest. We will refer to it as fine or high-fidelity model. The design task is formulated as a nonlinear minimization problem of the form

$$\boldsymbol{x}^* = \arg\min_{\boldsymbol{x}} U(\boldsymbol{R}_f(\boldsymbol{x})) \tag{1}$$

Here, $\boldsymbol{x}$ is a vector of designable parameters, whereas U is an objective function implementing given design specifications. $\boldsymbol{R}_f$ is assumed to be computationally expensive, which makes a direct optimization of $U(\boldsymbol{R}_f(\boldsymbol{x}))$ prohibitive.

2.2 Surrogate-Based Optimization

To solve (1), we exploit surrogate-based optimization (SBO) that generates a sequence of approximate solutions to (1), $\boldsymbol{x}^{(i)}$, $i = 0, 1, 2, \ldots$ as follows ($\boldsymbol{x}^{(0)}$ is an initial design) (Koziel *et al.*, 2012):

$$\boldsymbol{x}^{(i+1)} = \arg\min_{\boldsymbol{x}} U(\boldsymbol{R}_s^{(i)}(\boldsymbol{x})) \tag{2}$$

The surrogate model $\boldsymbol{R}_s^{(i)}$ is a fast representation of the fine model $\boldsymbol{R}_f$. In this work, $\boldsymbol{R}_s^{(i)}$ is created using a nested space mapping approach introduced in Section 2.3. The main rationale behind (2) is to shift the optimization burden into the surrogate model so that most of the operation (in particular, finding a new approximation of the optimum design $\boldsymbol{x}^*$) are performed on $\boldsymbol{R}_s^{(i)}$ rather than on $\boldsymbol{R}_f$. For a well working SBO algorithm, the number of iterations of (2) necessary to find a satisfactory solution is usually just a few. Also, the fine model is typically evaluated only once per iteration (Koziel *et al.*, 2012). The overall design optimization cost can be therefore dramatically reduced compared to conventional optimization.

2.3 Nested Space Mapping Modeling

The nested space mapping (NSM) technique proposed here is a two-level modeling methodology, with the first (inner) space mapping layer applied at the level of component, and the second (outer) layer applied at the level of the entire structure. The purpose of NSM is to improve the generalization capability of the surrogate model and facilitate the parameter extraction process. Consequently the cost of the design optimization process using NSM can be greatly reduced compared to conventional space mapping applied at the structure level only.

Figure 1 shows a typical CMRC component, its equivalent circuit representation, as well as a CMRC-based structure, here, a matching transformer. Let $\boldsymbol{R}_{f.cell}(\boldsymbol{y})$ and $\boldsymbol{R}_{c.cell}(\boldsymbol{y})$ denote the responses (here, S-parameters) of the fine (i.e., EM-simulated) and coarse (circuit-simulated) models of the CMRC component. The vector $\boldsymbol{y}$ represents geometry parameters of the component. $\boldsymbol{R}_f(\boldsymbol{x})$ and $\boldsymbol{R}_c(\boldsymbol{x})$ will stand for the fine and coarse models of the entire CMRC structure with $\boldsymbol{x}$ being a corresponding vector of geometry parameters.

The nested SM approach here builds up the surrogate model of the CMRC structure starting from the component level. We use $\boldsymbol{R}_{s.g.cell}(\boldsymbol{y},\boldsymbol{p})$ to denote a generic component surrogate, which is a composition of $\boldsymbol{R}_{c.cell}$ and suitable space mapping transformations; the vector $\boldsymbol{p}$ denotes the set of extractable SM parameters of the model. The SM surrogate $\boldsymbol{R}_{s.cell}$ of a CMRC component is obtained as

$$\boldsymbol{R}_{s.cell}(\boldsymbol{y}) = \boldsymbol{R}_{s.g.cell}(\boldsymbol{y}, \boldsymbol{p}^*) \tag{3}$$

The parameter vector $\boldsymbol{p}^*$ is obtained by solving the following nonlinear parameter extraction process

$$\boldsymbol{p}^* = \arg\min_{\boldsymbol{p}} \sum_{k=1}^{N_{cell}} \| \boldsymbol{R}_{s.g.cell}(\boldsymbol{y}^{(k)}, \boldsymbol{p}) - \boldsymbol{R}_f(\boldsymbol{y}^{(k)}) \| \tag{4}$$

The vectors $\boldsymbol{y}^{(k)}$, $k = 1, \ldots, N_{cell}$, denote the training (or base) designs. Here, we use the star-distributed base with $N_{cell} = 2n + 1$, where n is the number of designable parameters of the component of interest. For practical design cases (cf. Section 3), the generic component surrogate exploits a combination of input, implicit and frequency SM (Bandler *et al.*, 2004). The surrogate model $\boldsymbol{R}_{s.cell}$ is set up as a global model, i.e., it is supposed to be valid for the entire range of parameters $\boldsymbol{y}$ that will be used in the subsequent CMRC structure design.

We will denote by $\boldsymbol{R}_{s.g}(\boldsymbol{x},\boldsymbol{P})$ a generic space mapping surrogate of the entire MT, composed of the SM models of individual CMRC components, i.e., $\boldsymbol{R}_{s.g}(\boldsymbol{x},\boldsymbol{P}) = \boldsymbol{R}_{s.g}([\boldsymbol{y}_1; \ldots; \boldsymbol{y}_p],\boldsymbol{P}) = F(\boldsymbol{R}_{s.g.cell}(\boldsymbol{y}_1,\boldsymbol{p}^*),\ldots, \boldsymbol{R}_{s.g.cell}(\boldsymbol{y}_p,\boldsymbol{p}^*),\boldsymbol{P})$. For example, in case of matching transformers considered in Section 3, the function F realizes cascade connection of S-parameters of individual components; the parameter vector $\boldsymbol{x}$ is a concatenation of the component parameter vectors $\boldsymbol{y}_k$. The "global" SM parameter vector $\boldsymbol{P}$ is normally defined as perturbations (with respect to $\boldsymbol{p}^*$) of selected SM parameters of individual components.

The outer SM level is applied to the global model $\boldsymbol{R}_{s.g}(\boldsymbol{x},\boldsymbol{P})$, so that the final surrogate $\boldsymbol{R}_s^{(i)}$ utilized in the ith iteration of the SBO scheme (2) is defined as follows

$$\boldsymbol{R}_s^{(i)}(\boldsymbol{x}) = \boldsymbol{R}_{s.g}(\boldsymbol{x}^{(i)}, \boldsymbol{P}^{(i)}) \tag{5}$$

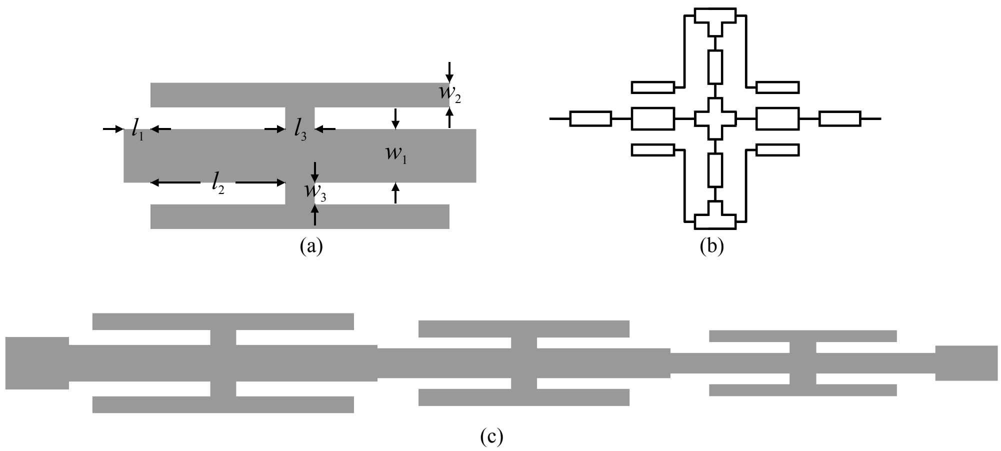

Figure 1: (a) Typical CMRC component (here, double-T), (b) its equivalent circuit, (c) exemplary CMRC-based structure (matching transformer).

where

$$\boldsymbol{P}^{(i)} = \arg\min_{\boldsymbol{P}} \| \boldsymbol{R}_{s.g}(\boldsymbol{x}^{(i)}, \boldsymbol{P}) - \boldsymbol{R}_f(\boldsymbol{x}^{(i)}) \| \tag{6}$$

It should be emphasized that in practice, the number of parameters in $\boldsymbol{P}$ is much smaller than the combined number of SM parameters of CMRC components (i.e., multiple copies of a vector $\boldsymbol{p}^*$). This is normally sufficient because the first SM layer already provides good alignment between the $\boldsymbol{R}_{s.cell}$ and $\boldsymbol{R}_{f.cell}$ so that the role of (5), (6) is mainly to account for possible couplings between CMRC components that are accounted for by the composing function F.

2.4 Generalization Capability of Nested Space Mapping. Optimization Algorithm Convergence

Figure 2 demonstrates typical modeling accuracy of the inner space mapping layer of NSM, illustrated here for a double-T CMRC-based component of Fig. 1(a). Globally accurate model at the CMRC component level obtained by (3), (4), ensures good generalization capability of the final NSM surrogate, which is the fundamental advantage of NSM. Figure 3 shows responses of the NSM surrogate before and after parameter extraction (PE) (5). The surrogate (i.e., $\boldsymbol{R}_{s.g}$) matches the fine model well even before PE. Parameter extraction is executed using only a few parameters and allows us to quickly compensate for the couplings between the CMRC components, which are not accounted for by the component models themselves. At the same time, NSM model exhibits excellent generalization as indicated in Fig. 3(b).

For the sake of comparison, conventional SM modeling of the entire transformer (i.e., correction of its coarse model $\boldsymbol{R}_c$) has been also performed. It is a much more complex process because (i) the coarse model of the entire transformer is much less accurate than $\boldsymbol{R}_{s.g}$ (cf. Fig. 4(a)), (ii) a large number of SM parameters is required, (iii) the parameter extraction process is more difficult and time consuming, and (iv) generalization capability of the model is poor (cf. Fig. 4(b)).

Sufficient accuracy of the underlying coarse model and good generalization capability of the surrogate are essential for fast convergence of the SBO optimization process (2) (Koziel *et al.*, 2008). The NSM model has both aforementioned features (here, the global model $\boldsymbol{R}_{s.g}$ is formally a coarse model for (2)), which results in rapid design of CMRC-based structures as demonstrated in the next section.

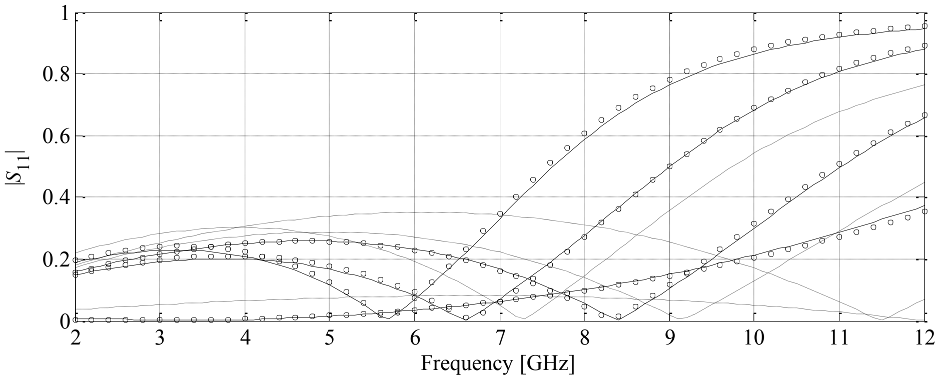

Figure 2: Nested space mapping modeling of a double-T CMRC component. Responses at the selected test designs: coarse model (····), fine model (—), NSM surrogate (o). The plots indicate very good approximation capability of the surrogate.

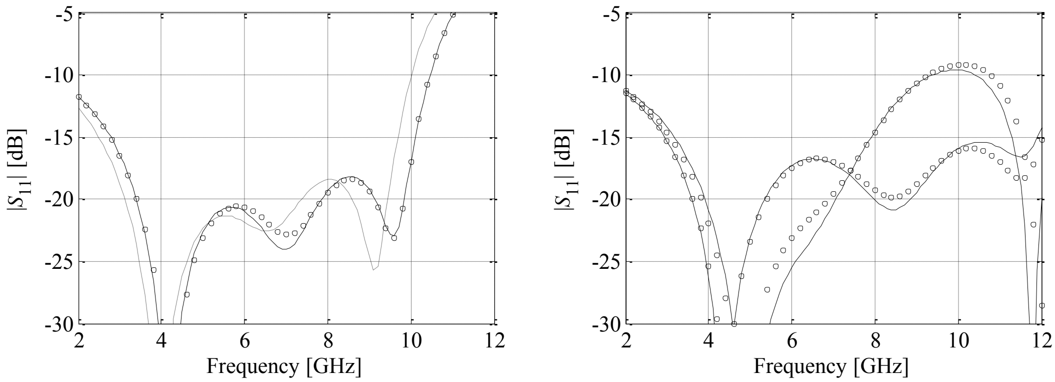

(a) (b)

Figure 3: Nested space mapping modeling of a double-T CMRC transformer: (a) fine (—), NSM surrogate before parameter extraction (····) and NSM surrogate after parameter extraction (o); (b) NSM surrogate extracted at the design of Fig. 4(a) shown at other designs (o) as well as corresponding fine model responses (—). Generalization capability of the NSM surrogate is very good.

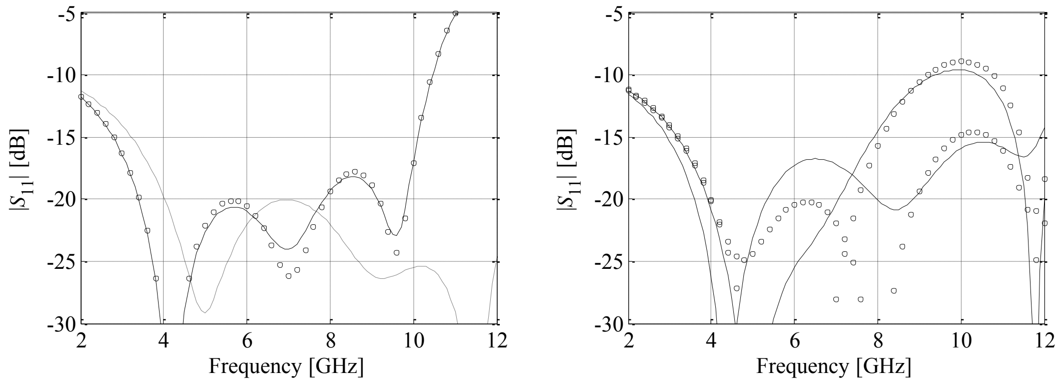

(a) (b)

Figure 4: Conventional space mapping modeling of a double-T CMRC transformer: (a) fine (—), SM surrogate before parameter extraction (····) and SM surrogate after parameter extraction (o); (b) SM surrogate extracted at the design of Fig. 4(a) shown at other designs (o) as well as corresponding fine model responses (—). Poor generalization capability of the conventional SM surrogate can be observed.

3 Case Study

In this section, we present verification results of the design optimization methodology of Section 2. Verification has been performed using the double-T CMRC component and matching transformers constructed using this component as a fundamental building block.

3.1 Surrogate Model Construction

The generic space mapping surrogate utilized in our numerical experiments takes the form of

$$\boldsymbol{R}_{s.g.cell}(\boldsymbol{y}, \boldsymbol{p}) = \boldsymbol{R}_{c.F}(\boldsymbol{B} \cdot \boldsymbol{x} + \boldsymbol{c}, \boldsymbol{p}_I) \tag{7}$$

where $\boldsymbol{B}$ and $\boldsymbol{c}$ are input SM parameters (here, we use diagonal matrix $\boldsymbol{B}$), $\boldsymbol{p}_I$ are implicit SM parameters (here, substrate parameters for individual microstrip models, specifically, dielectric permittivity and the substrate heights), as well as frequency scaling. $\boldsymbol{R}_{c.F}$ denotes frequency-scaled coarse model. Given that $\boldsymbol{R}_c$ describes evaluation of the same equivalent circuit model (cf. Fig. 1(b)) across a frequency band of interest, i.e., $\boldsymbol{R}_c(\boldsymbol{y}) = [R_c(\boldsymbol{y},\omega_1)\ \ R_c(\boldsymbol{y},\omega_2)\ \ldots\ R_c(\boldsymbol{y},\omega_m)]^T$, the frequency-scaled model is defined as

$$\boldsymbol{R}_{c.F}(\boldsymbol{y},\boldsymbol{p}) = [R_c(\boldsymbol{y}, f_0 + \omega_1 \cdot f_1)\ \ R_c(\boldsymbol{y}, f_0 + \omega_2 \cdot f_1)\ \ \ldots\ \ R_c(\boldsymbol{y}, f_0 + \omega_m \cdot f_1)]^T \quad (8)$$

where f_0, f_1 are extractable scaling parameters. Frequency scaling is very convenient to account for the frequency-like misalignment between the coarse and the fine model (such as frequency shifts).

3.2 Matching Transformer Structure and Optimization Results

A double-T structure (cf. Fig. 1(a)) is described by 4 geometric parameters $\boldsymbol{y} = [l_1\ l_2\ w_1\ w_2]^T$ (dimensions $l_3 = 0.2$ and $w_3 = 0.2$ are fixed). The high-fidelity models $\boldsymbol{R}_{f.cell}$ of the double-T structure and its coarse model $\boldsymbol{R}_{c.cell}$ are implemented in CST MWS (CST, 2013) (RF-35 substrate with $h = 0.76$ mm) and Agilent ADS (ADS, 2011), respectively.

The first layer of the NSM model is created using 16 space mapping parameters, including eight parameters of input SM, two frequency scaling parameters, and six implicit SM parameters. The quality of the extracted CMRC component model has been illustrated in Fig. 2.

Consider a cascade of double-T CMRC components, Fig. 1(c), used for a construction of 3- and 4-section MTs. The design objective is to achieve $|S_{11}| \le -15$ dB in UWB band (3.1 to 10.6 GHz). The vector of initial design parameters of each section is: $\boldsymbol{y} = [0.65\ 0.35\ 0.55\ 3.75]^T$.

A 3-section MT (i) is designed to match 50Ω÷100Ω impedance. The final design: $\boldsymbol{x} = [0.5\ 4.36\ 0.76\ 0.2\ 0.5\ 3.73\ 0.49\ 0.2\ 0.5\ 3.22\ 0.24\ 0.2]^T$ is obtained after 2 iterations of the NSM technique ($|S_{11}| \le -17.5$ dB for 3.1 GHz to 10.6 GHz).

A cascade of 4 cells, constitutes a 50Ω÷130Ω MT (ii). The final MT design denoted by: $\boldsymbol{x} = [1.0\ 3.52\ 0.85\ 0.2\ 0.8\ 4.10\ 0.58\ 0.05\ 0.8\ 3.09\ 0.1\ 0.25\ 1\ 2.315\ 0.13\ 0.05]^T$ is obtained after only 3 iterations of the proposed algorithm ($|S_{11}| \le -16.5$ dB for 3.1 GHz to 10.6 GHz).

One should emphasize that for both MTs, the number of the outer layer SM parameters $\boldsymbol{P}$ is much smaller than the combined set of SM parameters for the inner layer (11 vs. 48 for the first MT and 14 vs. 64 for the second one) as only frequency scaling and selected implicit SM parameters are used. Reduction of the number of parameters (possible because of excellent generalization capability of NSM) considerably speeds up the design process. The reflection characteristics of (i) and (ii) MTs are shown in Fig. 5.

3.3 Comparisons

The computational efficiency of NSM was compared with implicit space-mapping (Bandler *et al.*, 2004) and sequential space-mapping (Bekasiewicz *et al.*, 2012) that were previously used for CMRC-based structure design. The proposed technique results in the smallest number of iterations necessary to yield an optimized geometry (see Table 1) for all considered cases. Additionally, a comparison with direct optimization of the EM transformer model is included, here, using pattern search (Kolda *et al.*, 2003) to show that the latter method is virtually impractical for the design of compact MTs.

4 Conclusions

A nested SM (NSM) optimization technique has been presented. In our approach, a two-layer space mapping model is constructed, with the inner layer applied at the component level, and the outer layer applied at the level of the entire structure under design. The fundamental advantage of the proposed technique is the generalization capability of the NSM surrogate is significantly better than that of the conventional (single-layer) space mapping model, which leads to a decreased overall design cost, a reduced number of extractable surrogate model parameters, and improving the robustness of the optimization process. NSM is validated using two test cases. In both cases, the average optimization cost is three iterations or less. This is a significant speedup compared to competitive surrogate-based methods, leaving alone direct optimization of the EM-simulation model.

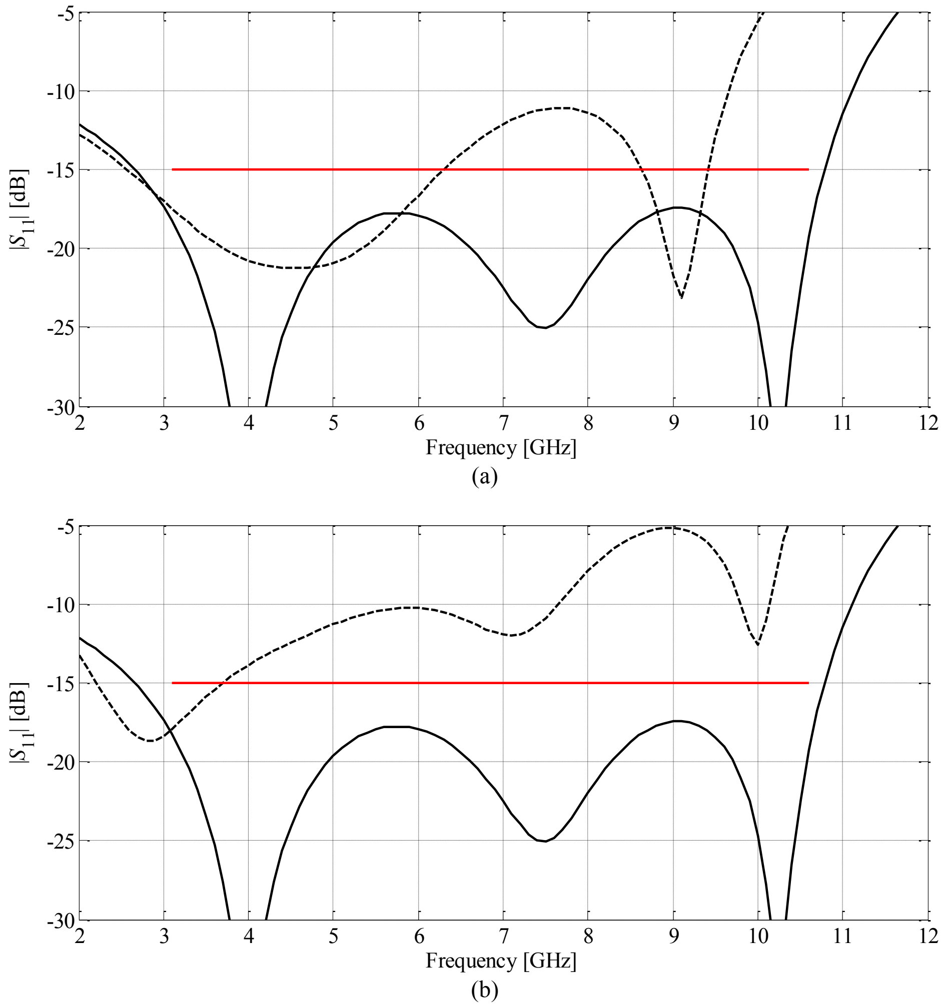

Figure 5: Reflection responses of the optimized matching transformers: (a) transformer (i) at the initial (- - -) and at the optimized (—) design; (b) transformer (ii) at the initial (- - -) and at the optimized (—) design.

SBO method	Design Cost (number of EM simulations)	
	MT (i)	MT (ii)
Nested SM (this work)	2	3
Implicit SM (Bandler *et al.*, 2004)	8	9
Sequential SM (Bekasiewicz *et al.*, 2012)	7	10#
Direct Search	406	500*

Table 1: Design optimization cost (# the algorithm started diverging and was terminated after 10 iterations; * The algorithm failed to find a geometry satisfying performance specifications)

References

Agilent ADS (2011), Agilent Technologies, 1400 Fountaingrove Parkway, Santa Rosa, CA 95403-1799.

Bandler, J.W., Cheng, Q.S., Dakroury, S.A., Mohamed, A.S., Bakr, M.H., Madsen, K., Søndergaard, J. (2004) *Space mapping: the state of the art*. IEEE Trans. Microwave Theory Tech., 52, 337−361.

Bekasiewicz, A., Kurgan, P. (2014) *A compact microstrip rat-race coupler constituted by nonuniform transmission lines*. To appear Microwave and Opt. Technology Lett.

Bekasiewicz, A., Kurgan, P., Kitlinski, M. (2012) *New approach to a fast and accurate design of microwave circuits with complex topologies*. IET Microwaves, Antennas & Prop., 6, 1616-1622.

Cheng, Q.S., Koziel, S., Bandler, J.W. (2006) *Simplified space mapping approach to enhancement of microwave device models*. Int. J. RF and Microwave Computer-Aided Eng., 16, 518-535.

Chuang, M.-L., Wu, M.-T. (2004) *Miniaturized ring coupler using multiple open stubs*. Microwave and Opt. Technology Lett., 42, 379-383.

CST Microwave Studio (2013). CST AG, Bad Nauheimer Str. 19, D-64289 Darmstadt, Germany.

Forrester, A.I.J., Keane, A.J. (2009) *Recent advances in surrogate-based optimization*. Prog. in Aerospace Sciences, 45, 50−79.

Kolda, T.G., Lewis, R.M., and Torczon, V. (2003) *Optimization by direct search: new perspectives on some classical and modern methods*. SIAM Review, 45, 385-482.

Koziel, S., Bandler, J.W., Madsen, K. (2006) *A space mapping framework for engineering optimization: theory and implementation*. IEEE Trans. Microwave Theory Tech., 54, 3721-3730.

Koziel, S., Bandler, J.W., Madsen, K. (2008) *Quality assessment of coarse models and surrogates for space mapping optimization*. Optimization Eng. 9, 375-391.

Koziel, S., Echeverría-Ciaurri, D., Leifsson, L. (2011) *Surrogate-based methods*, in S. Koziel and X.S. Yang (Eds.) *Computational Optimization, Methods and Algorithms*, Series: Studies in Computational Intelligence, Springer-Verlag, pp. 33-60.

Koziel, S., Ogurtsov, S. (2012) Model management for cost-efficient surrogate-based optimization of antennas using variable-fidelity electromagnetic simulations. IET Microwaves Antennas Prop., 6, pp. 1643-1650.

Koziel, S., Leifsson, L., and Yang, X.S. (2012) *Surrogate-based optimization*. In S. Koziel, X.S. Yang, Q.J. Zhang (Eds.) *Simulation-Driven Design Optimization and Modeling for Microwave Engineering*, Imperial College Press, 41-80.

Koziel, S., Leifsson, L., Ogurtsov, S. (2013a) *Space Mapping for Electromagnetic-Simulation-Driven Design Optimization*. In S. Koziel, L. Leifsson (Eds.) *Surrogate-Based Modeling and optimization: Applications in Engineering*, Springer, 1-27.

Koziel, S., Leifsson, L., Ogurtsov, S. (2013b) *Reliable EM-driven microwave design optimization using manifold mapping and adjoint sensitivity*. Microwave and Opt. Technology Let., 55, 809-813.

Kurgan, P., Filipcewicz, J., Kitlinski, M. (2012) *Development of a compact microstrip resonant cell aimed at efficient microwave component size reduction*. IET Microwaves, Antennas Prop., 6, 1291-1298.

Kurgan, P., Kitlinski, M. (2009) *Novel doubly perforated broadband microstrip branch-line couplers*. Microwave Opt. Technology Lett., 51, 2149-2152.

Kurgan, P., Kitlinski, M. (2010) *Slow-wave fractal-shaped compact microstrip resonant cell*. Microwave Opt. Technology Lett., 52, 2613-2615.

Kurgan, P., Bekasiewicz, A. (2014) *A robust design of a numerically demanding compact rat-race coupler*. To appear Microwave Opt. Technology Lett.

Smierzchalski, M., Kurgan, P., Kitlinski, M. (2010) *Improved selectivity compact band-stop filter with Gosper fractal-shaped defected ground structures*. Microwave Opt. Technology Let., 52, 227-232.

Tsai, L.-T. (2013) *A compact dual-passband filter using stepped-impedance resonators*, Microwave Opt. Technology Lett., 55, 2514-2517.

Wincza, K., Gruszczynski, S. (2013) *Theoretical limits on miniaturization of directional couplers designed as a connection of tightly coupled and uncoupled lines*, Microwave Opt. Technology Lett., 55, 223-230.